

Fabrication of Superhydrophobic Fiber Coatings by DC-Biased AC-Electrospinning

Fredrick O. Ochanda, Mohamed A. Samaha, Hooman Vahedi Tafreshi, Gary C. Tepper, Mohamed Gad-el-Hak

Department of Mechanical & Nuclear Engineering, Virginia Commonwealth University, Richmond, Virginia 23284-3015

Received 4 February 2011; accepted 25 March 2011

DOI 10.1002/app.34583

Published online 9 August 2011 in Wiley Online Library (wileyonlinelibrary.com).

ABSTRACT: Mesh-like fiber mats of polystyrene (PS) were deposited using DC-biased AC-electrospinning. Superhydrophobic surfaces with water contact angles greater than 150° and gas fraction values of up to 97% were obtained. Rheological study was conducted on these fiber surfaces and showed a decrease in shear stress when compared with a noncoated surface (no slip), making them excellent candidates for applications requiring the reduction of skin-friction drag in submerged surfaces. We have also shown that addition of a second, low-surface energy polymer to a solution of PS can be used to control the fiber inter-

nal porosity depending on the concentration of the second polymer. Contact-angle measurements on mats consisting of porous and nonporous fibers have been used to evaluate the role of the larger spaces between the fibers and the pores on individual fibers on superhydrophobicity. © 2011 Wiley Periodicals, Inc. *J Appl Polym Sci* 123: 1112–1119, 2012

Key words: superhydrophobic surfaces; electrospinning; DC-biased AC-electrospinning; superhydrophobic fibrous coatings; fabrication and characterization of superhydrophobic surfaces

INTRODUCTION

Superhydrophobicity is achieved by combining nano- or microscale roughness with a low-surface free energy material. As water flows over such a surface, a “slip effect” is generated, resulting in a reduction in the skin-friction drag exerted on the surface.¹ Several methods have been used to fabricate superhydrophobic surfaces, including sol-gel processing² and solution casting,³ chemical vapor deposition,⁴ laser/plasma/chemical etching,⁵ lithography,⁶ electrical/chemical reaction and deposition,⁷ layer-by-layer and self-assembly,⁸ and electrospinning. Except for the last, all of these methods are complicated and require special equipment, high temperature or vacuum conditions, or low-surface energy material modification involving multiple steps, which makes it difficult for practical applications in large-scale coatings.

Electrospinning is a simple, low-cost method that can be used to deposit micro- to nanotextured coatings of a hydrophobic polymer onto substrates of arbitrary geometry. The resulting superhydrophobic surfaces can be applied in diverse applications, including self-cleaning glasses and clothes, protection against corrosion of metallic parts (in bridges,

marines, under water constructions, etc.), antisnow sticking, and reducing skin-friction drag in underwater vessels such as submarines. Superhydrophobic coatings can be utilized as a passive method of flow control and may potentially become a viable alternative to the more complex and energy consuming active or reactive flow control techniques such as wall suction/blowing.⁹ Conventionally, electrospinning is performed by applying a large DC-potential between the electrospinning source (typically a hypodermic syringe) and the substrate, resulting in a randomly oriented nonwoven fiber mats. The random orientation of the fibers is the result of the inherent electrostatic instability of the charged jet as it travels from the spinneret to the collection substrate. This instability can be overcome by applying a DC-biased AC-potential that induces short segments of alternating polarity, thereby reducing the magnitude of the destabilizing force on the fiber.¹⁰ In addition, the presence of both positive and negative charges on the surface of the rotating collector minimizes the local electric field perturbations caused by residual charge accumulation on the fibers.

Different groups have fabricated superhydrophobic surfaces using electrospinning and other wet chemical approaches.^{11–13} Sun and coworkers¹⁴ demonstrated the preparation of superhydrophobic, anisotropically aligned carbon nanotube films by chemical vapor deposition on silicon substrates with quadrate micropillar arrays prepared by photolithography. Grid-like “nanoglass” and “nanobrick”

Correspondence to: M. Gad-el-Hak (gadelhak@vcu.edu).

TABLE I
DC-Biased AC-Electrospinning Conditions

AC voltage	DC voltage	Average voltage	Frequency	% duty	Pump rate	Nozzle–Shaft distance
11 kV _{p-p}	4.8 kV	4.8 kV	500 Hz	50	0.9 mL/h	5–7 cm

superhydrophobic surfaces fabricated lithographically at Bell Laboratories have also been reported.¹⁵ However, these surfaces made from silicon posts had to be coated with a hydrophobic material to impart superhydrophobic characteristics. Their skin-friction tests showed drag reduction due to air trapped between the posts and grids. Wang et al.¹⁶ also fabricated a superhydrophobic copper mesh by knitting copper wire, followed by the deposition of copper clusters and long-chain fatty acids.

Although superhydrophobic surfaces consisting of mats of randomly oriented, nonwoven electrospun fibers have been reported, at this time, the effect of fiber orientation on surface hydrophobicity has not previously been investigated. Recently, Tepper and coworkers¹⁰ showed that DC-biased AC-electrospinning can be used to prepare aligned 1-D polymer nanofibers, but no superhydrophobic studies were performed on these polymer fibers. Within this article, we describe a method for fabricating orthogonal, superhydrophobic fiber coatings using a single step approach. To the best of our knowledge, this is the first example in which mesh-like (grid-like) superhydrophobic fiber surfaces have been fabricated using electrospinning. Contact-angle measurements were performed on coatings consisting of porous and nonporous fibers, and the fiber porosity had no observable effect on superhydrophobicity, indicating that the air gaps between the fibers and not the internal fiber porosity are responsible for the observed superhydrophobicity. We further show that hydrophobicity can be controlled by varying the percent weight of the polymer in the electrospun solution.

EXPERIMENTAL APPROACH

Hydrophobic polymer, polystyrene (PS; $M_n = 170,000$), was purchased from Sigma-Aldrich Chemicals (St. Louis, Missouri) and used as received. *N,N*-Dimethylformamide (DMF) and toluene at high performance liquid chromatography grade were also obtained from Sigma-Aldrich and were used without further purification. Polymer fibers were fabricated using the DC-biased AC-electrospinning technique. The fibers were electrospun from solutions with 15, 18, 20, 25, and 30 wt % PS. The polymer was first dissolved in a solvent mixture of DMF and toluene with a 1 : 1 weight ratio. In addition, other additives such as glass beads and fluoro-elastomer (Zonyl TBC) were added to the electrospinning solutions to deter-

mine their effect on hydrophobicity. Electrospinning was conducted at 22°C with a relative humidity of 45% and a solution feed rate of 0.9 mL/h, controlled using a syringe pump. The fibers were collected by a rotating shaft at a distance of 5–7 cm from the spinneret. Directional fiber bundles were obtained from a rotational shaft collector at a tangential velocity from 23 to 30 m/s. A function generator was used to generate the AC signal in the form of a square wave at selected frequency, amplitude, and duty cycle. A high voltage amplifier with ± 10 kV_{ac} and frequency range of DC to 30 kHz was employed to amplify the output of the function generator by biasing the AC voltage to an optimum DC value. The fibers were collected on the substrate for a specified amount of time and then rotated about 90° for the same specified amount of time to generate a grid-like geometry. The experimental conditions for the electrospinning process are summarized in Table I.

The static contact angles, a measure of surface hydrophobicity, were measured using a contact-angle ramé-hart goniometer and droplets of deionized water on the specimen. Droplets of about 3 μ L in volume (diameter of about 1.8 mm) were gently deposited on the substrate using a microsyringe. All measurements were made at five different points for each sample at $20 \pm 1^\circ\text{C}$. An image of the droplet was taken by an F1 Series Digital Camera and transferred to a PC for contact-angle determination. The morphology of the fiber and its surface structure were observed by field emission scanning electron microscopy (FESEM; S-70, Hitachi, Japan). Because of the nonconductivity of our samples and to minimize the charging effects, the samples were sputter-coated with gold–palladium at a set point of 35 mA for 60 s. The gold–palladium coating's thickness under those conditions was 50 nm. The acceleration voltage and working distance for each image were 5 kV and 10 mm, respectively. Finally, rheological experiments in parallel-plate geometry were performed on an MCR 300 (Paar Physica).

RESULTS AND DISCUSSION

Effect of surface morphology on superhydrophobic coatings

Using a DC-biased AC-potential to charge the solution performs two functions. The electrospinning jet from the DC-biased AC-potential consists of short segments of alternating polarity which significantly

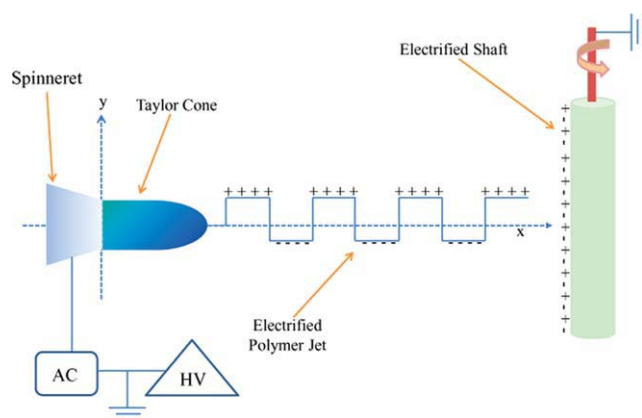


Figure 1 An illustration of an electrified polymer jet during a DC-biased AC-electrospinning. [Color figure can be viewed in the online issue, which is available at wileyonlinelibrary.com.]

reduces the inherent instability of the electrospinning jet as shown in Figure 1. This allows the fibers to be wound onto the rotating collector with greater ease and alignment. The presence of both positive and negative charges on the surface of the rotating collector minimizes the local electric fields associated with surface charge accumulation. The deposited mat of hydrophobic polymer fibers provides the surface roughness and porosity necessary to entrap air when the surface is immersed in water. As water flows over this surface, the interface between the entrapped air and the water has very low skin friction, resulting in slip flow and drag reduction. The grid-like arrangement of fibers prevents liquid from wetting into the space (pitch) between fiber posts, similar to microposts made by a microfabrication method. This requires that the fiber post spacing be close enough (typically micrometers) to counteract gravitational and other pressures that might cause wetting into the space between the posts. However,

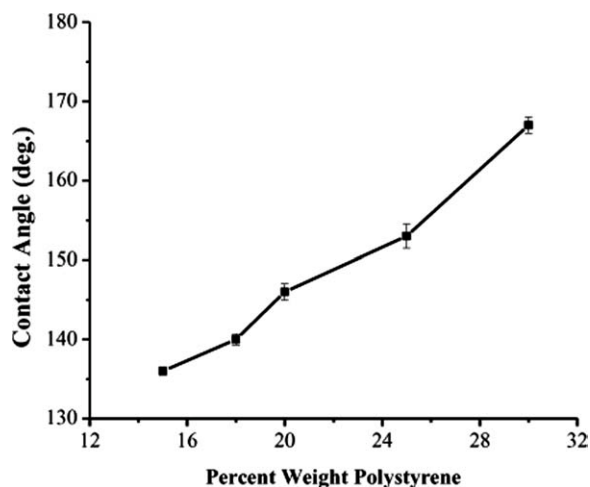


Figure 2 Water contact angles of electrospun fibers as a function of percent weight polystyrene.

if superhydrophobicity is to be achieved, the fraction of the water droplet surface that contacts the low-surface energy posts should be much less than the fractional area of the water droplet contacting the air. The grid-like geometry of fibers has the advantage of careful control of the pitch, but with additional microscale surface roughness on the posts in a single step that further increases the hydrophobicity. Compared with a random fiber geometry, a grid-like fiber geometry results in well-controlled, high void volume, and high porosity. Furthermore, the roughness details and the void volume can be controlled at a dimension much smaller than the droplet size. Examining the dimension of the pitch (25–80 μm), the typical droplet size reported here (1.8 mm) is more than an order of magnitude larger.

The effect of percent weight of PS on the hydrophobicity of electrospun fiber coatings was investigated. Figure 2 is a plot of the contact angle versus the percent weight of the polymer. The contact angle increases monotonically with polymer weight percent and becomes superhydrophobic at 25 wt %. This is consistent with the observed morphological evolution as a function of polymer concentration. At low percentage weight, electrospinning generates predominantly droplets (particles) with very few fibers. With an increase in polymer concentration, more fibers are generated with a few cases of beads-on-string morphology. At an optimum concentration, the ratio of fibers to beads should give the highest superhydrophobicity. Images of water droplets on fiber surfaces at different percentage polymer weight are shown in Figure 3.

The addition of glass particles of size 5 μm has resulted in an increase in contact angle on the 18 wt %

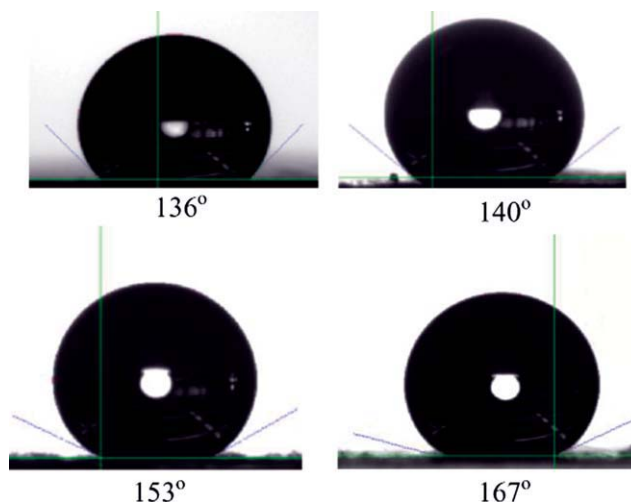


Figure 3 Contact angles of fibers as a function of percent weight of polystyrene. From left to right, top to bottom: 15 wt %, 18 wt %, 25 wt %, and 30 wt %. [Color figure can be viewed in the online issue, which is available at wileyonlinelibrary.com.]

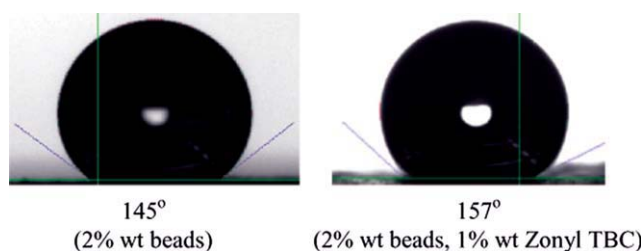


Figure 4 A water droplet on 18 wt % polystyrene fibers coating. [Color figure can be viewed in the online issue, which is available at wileyonlinelibrary.com.]

PS fiber coating from 140° to 145°. When 1 wt % fluoro-elastomer (Zonyl TBC) was added to the 18 wt % PS solution with glass particles, a large increase in contact angle was observed (157°) as shown in Figure 4. This could be ascribed to a decrease in surface energy as a result of the fluoro-elastomer (Zonyl TBC), which also increased the solution concentration of the PS blend. The addition of glass particles to 25 wt % solution also resulted in an increase in the contact angle from 153° to 160° (see Fig. 5). However, there was a slight decrease in contact angle when glass particles were added to 30 wt % PS coating from 167° to 156° (see Fig. 6). Further decrease in contact angle occurred with the addition of epoxyhexylisobutyl POSS (polyhedral oligomeric silsesquioxane) with a water contact angle of 150°. The decrease in contact angle when POSS is added to PS can be attributed to the epoxy functionality of the POSS that might have altered the surface energy of the PS coating. The effect of different additives on the hydrophobicity of electrospun PS fibers is summarized in Table II.

To measure the intrinsic hydrophobicity of PS, the polymer was dissolved in a DMF/toluene mixed solvent (1 : 1) at a concentration of 15 wt %. A PS thin film was fabricated by spin-casting on a microscope glass. The water contact angle of the spin cast PS film was determined to be $96.9 \pm 1.1^\circ$ and an optical image of the droplet is shown in Figure 7. Based on this we conclude that PS is chemically hydrophobic (water contact angle was higher than 90°) but is not superhydrophobic without surface roughness. The superhydrophobic coatings shown in Figure 9 are a

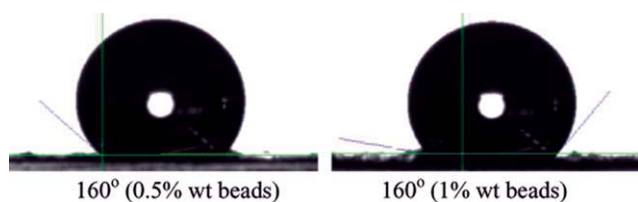


Figure 5 A water droplet on 25 wt % polystyrene fibers coating. [Color figure can be viewed in the online issue, which is available at wileyonlinelibrary.com.]

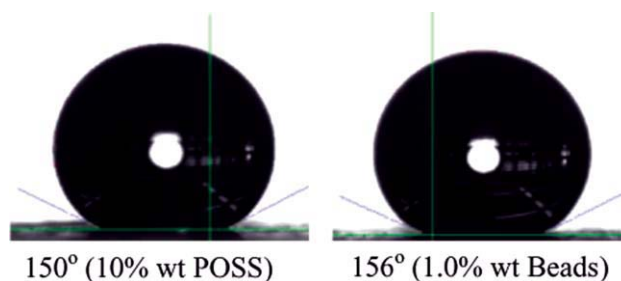


Figure 6 A water droplet on 30 wt % polystyrene fibers coating. [Color figure can be viewed in the online issue, which is available at wileyonlinelibrary.com.]

result of the web-like structure with empty spaces between the fibers.

To fully understand the hydrophobicity of the PS electrospun fiber surface, theoretical considerations are necessary. The contact angle on a composite surface (θ_r) can be expressed by Cassie and Baxter equation.^{17–19}

$$\cos \theta_r = f_1 \cos \theta - f_2$$

In this equation, f_1 and f_2 represent the fractions of solid surface and air in a composite surface, respectively (i.e., $f_1 + f_2 = 1$), whereas θ is the equilibrium contact angle on a flat, solid surface. This equation can be used to show that an increase in air fraction, f_2 , results in an increase in contact of the PS fiber surface. We measured the water contact angle on different PS fiber surfaces. The average contact angle on the different porous PS fiber surfaces has been summarized in the Table II. These values, together with the contact angle of a smooth PS film, made by spin coating a PS solution, have been used to estimate f_2 . The f_2 value for different PS fiber surfaces (i.e., different percent weight PS) is shown in Table III. It should be noted from the Table that the film of air occupies about 68–97% of the contact area (solid–

TABLE II
Effect of Additives on the Hydrophobicity of Polystyrene Fibers at Different Percent Weight Polystyrene

Case	wt % PS	wt % glass beads	wt % zonyl TBC	wt % POSS	Contact angle (deg.)
1	15	—	—	—	136
2	18	—	—	—	140
2	18	2.0	—	—	145
2	18	2.0	1.0	—	157
3	25	—	—	—	153
3	25	0.5	—	—	160
3	25	1.0	—	—	160
3	25	—	—	10	152
4	30	—	—	—	167
4	30	1.0	—	—	156
4	30	—	—	10	150

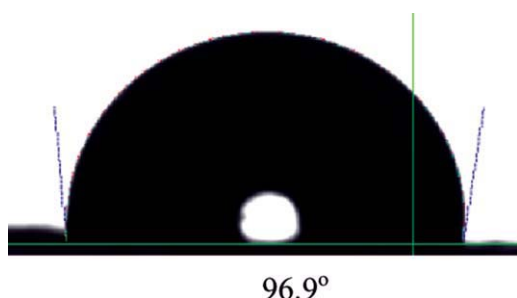


Figure 7 Contact angle of spin cast 15 wt % PS thin film. [Color figure can be viewed in the online issue, which is available at wileyonlinelibrary.com.]

liquid interface) when the fiber surface is in contact with the water droplet. This is responsible for the superhydrophobicity of the surface.

Electrospun fiber morphology

PS mats were produced by electrospinning from solutions with concentrations ranging from 18 to 30 wt % PS as shown in Figures 8–11. The electrospun fibers obtained from a solution containing PS and Toluene/DMF (1 : 1, w/w) were orthogonally oriented and each fiber had an average diameter of $2.5 \pm 1.2 \mu\text{m}$ ($N = 60$), a flat surface with irregular pores of diameter $500 \pm 100 \text{ nm}$ ($N = 60$) and regular pores of diameter $150 \pm 50 \text{ nm}$, as reported by Rabolt and coworkers.^{20,21} This porous morphology results from the different evaporation fronts of the mixed solvents and the phase separation of the polymer in the mixed solvents, during electrospinning.

The surface morphology of the electrospun PS fibers shows continuous and oriented electrospun fibers with uniform cylindrical pores and large-scale grooves along the individual fibers. These figures also show that the surface of the PS electrospun fibers is rough enough that air can be present in between individual fiber layers. The coatings shown

TABLE III
Estimate of Air Fraction on Composite Surface in Contact with Droplet from Cassie–Baxter Equation

Case	Percent weight PS	Contact angle (deg.)	Air fraction
1	15	136	68.0
2	18	140	73.4
2	18 (+2% glass beads)	145	79.5
2	18 (+2% glass beads + 1% fluoro-elastomer)	157	91.0
3	25	153	87.5
3	25 (+10% POSS)	152	86.7
3	25 (+1% glass beads)	160	93.0
4	30	167	97.0
4	30 (+1% glass beads)	160	93.0
4	30 (+10% POSS)	150	85.0

here can be regarded as a composite surface consisting of fibers and air. Both of the nonwoven electrospun membranes had a rougher surface morphology than the spin cast films. As a result, they were found to have a much higher water contact angle. It is revealed that micro- and nanoscale hierarchical structures on the PS fiber mesh play an important role in obtaining the unique superhydrophobic property. This electrospinning approach has the benefit of introducing different pore structures and hence achieving hierarchical surfaces in a single step.

The addition of a second polymer to a solution of PS has been shown to change the porosity of the resulting fibers, as illustrated by Figure 8, where pores and grooves along the single fiber have been eliminated. This feature has no effect on the superhydrophobicity of this sample, which proves that the large porous network resulting from the air caught in the spaces between fibers is responsible for superhydrophobicity, and that pores on individual fibers play a minimal role. This phenomenon has been verified further by making an 18% PS with 0.5% of fluoro-elastomer composite and observing the trend from the scanning electron microscopy

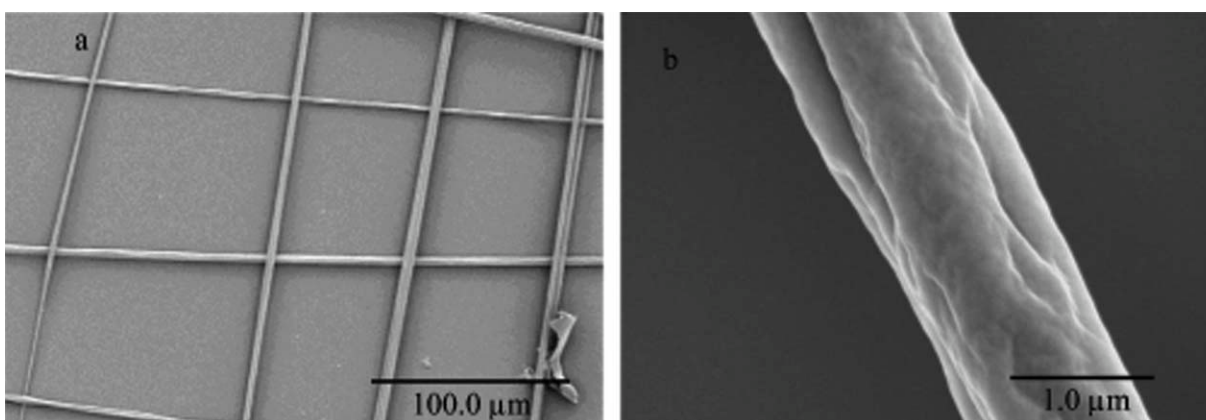


Figure 8 SEM image of 18 wt % polystyrene fibers with 1 wt % fluoro-elastomer and 2% glass beads showing (a) grid-like structure and (b) high magnification of single fiber.

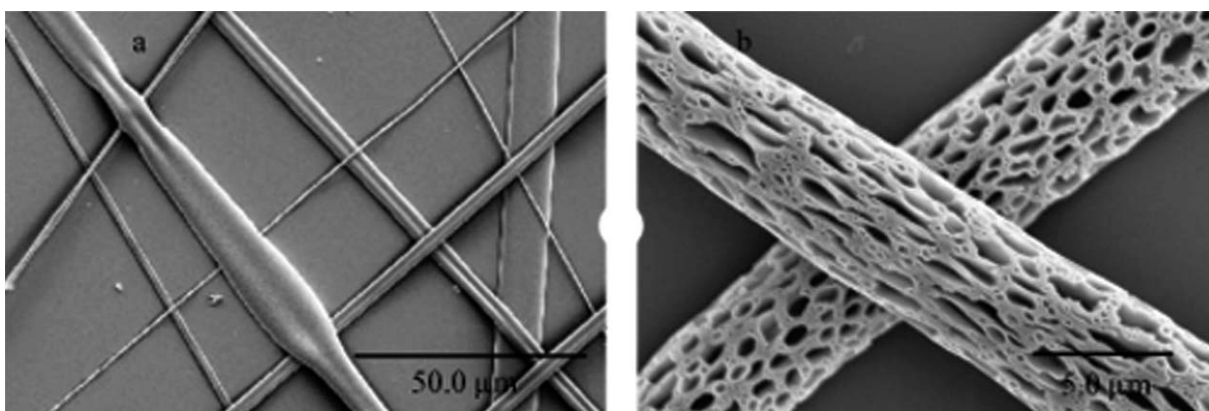


Figure 9 SEM image of 20 wt % polystyrene fibers showing (a) grid-like structure and (b) high magnification of single fiber exhibiting porous network.

(SEM) image shown in Figure 12. From the image, the pores are incompletely filled when compared with the case of 18% PS with 1.0% fluoro-elastomer. This observation shows that morphology and surface features of the electrospun fibers can be controlled by the addition of a small percent weight of a second polymer. Therefore, we conclude that a minimum concentration of fluoro-elastomer is required to completely eliminate the fiber pores. This ability to control the morphology of fiber coatings using DC-biased AC-electrospinning makes this fabrication approach very attractive for preparing surfaces for different applications.

Rheology of mesh-like superhydrophobic fiber coatings

A rheometer made by Anton Paar Corp. (model number MCR 300), equipped with two parallel rotating discs separated by a small fluid-filled gap, was used to measure the stress-strain rate relation. One disc is stationary and attached to a water cooling system for temperature control. The second disc

rotates at a prescribed speed and is connected to an air bearing to minimize friction. Compressed air at about 6 atm supports the bearing. The rotating disc is connected to a torque-speed measuring system used to calculate the shear stress developed by the fluid, and the measured rotational speed is used to calculate the strain rate. The stress-strain rate relation was measured for both superhydrophobic samples as well as smooth control surfaces. The test samples were attached to the stationary disc and had the same diameter as the rotating disc. Figure 13 shows the measured stress-strain curve for a non-coated disc (no slip), a superhydrophobic surface produced by the DC-biased AC-electrospinning technique.

The results show that the electrospun superhydrophobic PS fiber coating has lower shear stress than a noncoated disc (no slip). This result is consistent with the high contact-angle measurements, which indicate that the fluid in contact with the surface is also in contact with the trapped air, enabling the water layer to roll or slip. This phenomenon of low viscous friction on the superhydrophobic fiber

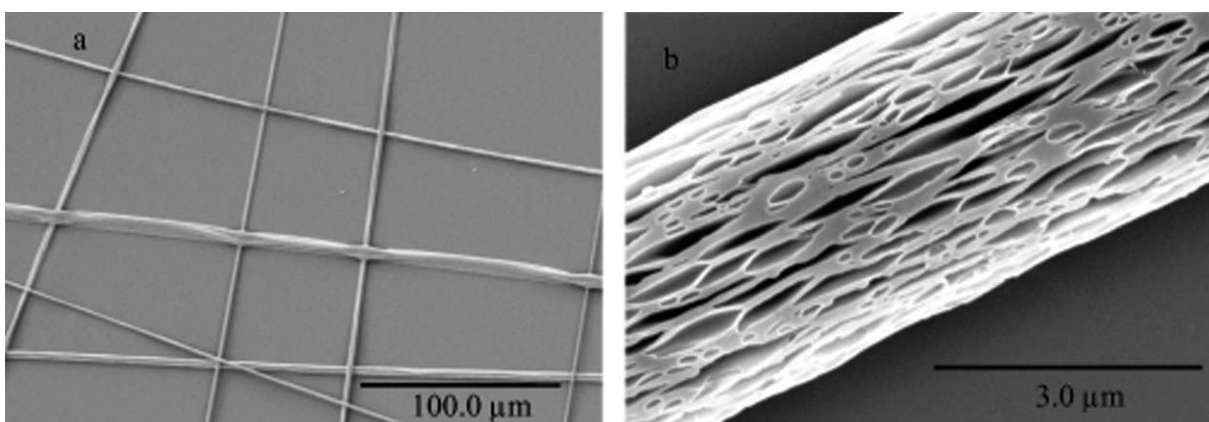


Figure 10 SEM image of 25 wt % polystyrene fibers showing (a) grid-like structure and (b) high magnification of single fiber exhibiting porous network.

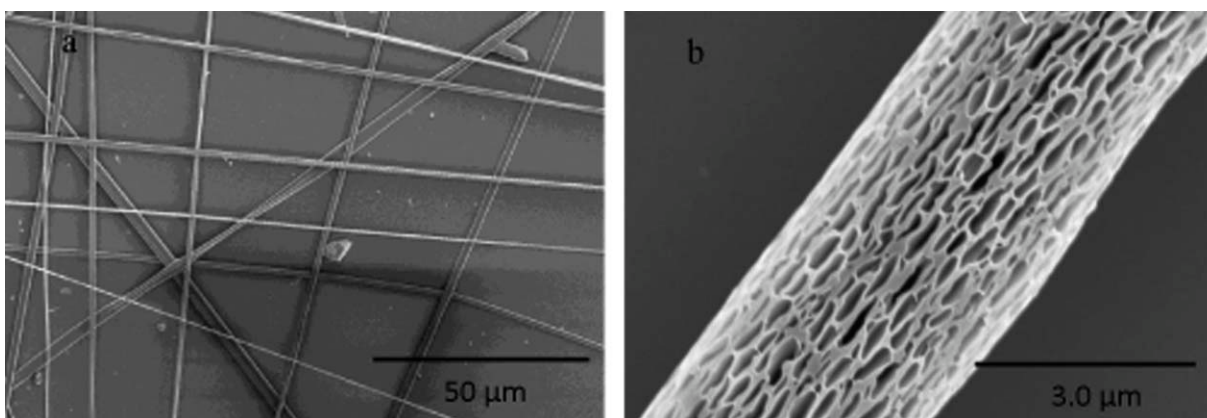


Figure 11 SEM image of 30 wt % polystyrene fibers showing (a) grid-like structure and (b) high magnification of single fiber exhibiting porous network.

surfaces is expected to open new opportunities for drag reduction in underwater bodies, especially submarines. A more detailed rheological study of the superhydrophobic electrospun fibers is under way.

CONCLUSIONS

Mesh-like PS fibers were synthesized by a simple DC-biased AC-electrospinning process and deposited onto metal substrates. The synthesized fibers were found to be superhydrophobic, with water contact angles up to 167° . These fiber coatings are far less expensive to fabricate when compared with those made with micro- or nanofabrication techniques. These results confirm that the physical surface structure is an important element affecting the surface hydrophobicity, in addition to the intrinsic hydrophobicity of materials such as PS. Rheological study conducted on these grid-like fiber surfaces showed a decrease in shear stress when compared with a noncoated surface (no slip). These surfaces

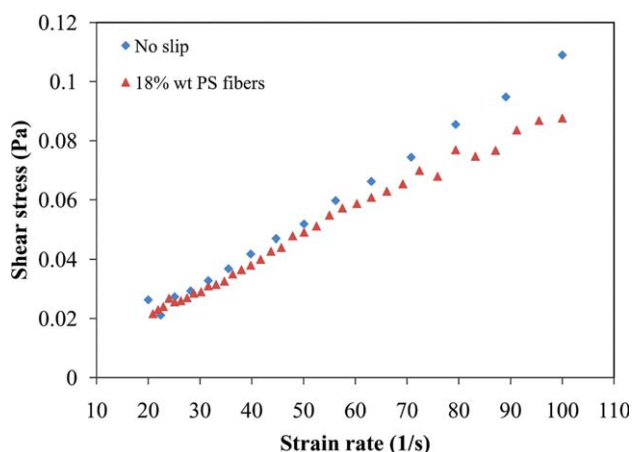


Figure 13 Plot of stress–strain curve of 18 wt % polystyrene fiber surface containing 1 wt % fluoro-elastomer. The figure shows lower shear stress when compared with no-slip surface. [Color figure can be viewed in the online issue, which is available at wileyonlinelibrary.com.]

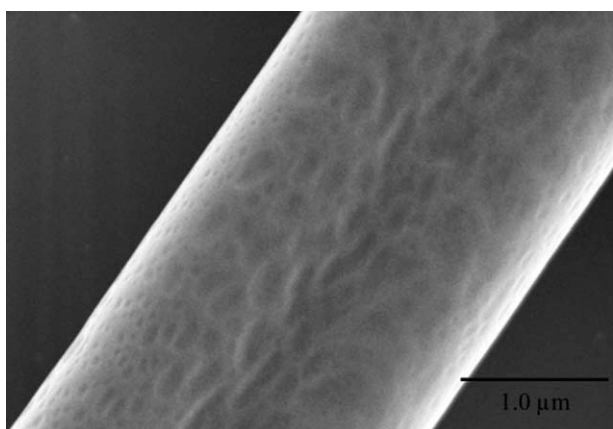


Figure 12 SEM image of 18 wt % polystyrene with 0.5 wt % fluoro-elastomer showing partially filled pores along the fiber.

are expected to have potential applications in submarine and ship coatings for the purpose of reducing of skin-friction drag and flow-induced noise. We have also shown that the addition of a second, low-surface energy polymer to a solution of PS can be used to control the internal porosity of the fibers, depending on the concentration of the second polymer. Contact-angle measurements indicated no effect on the superhydrophobicity on addition of second polymer, an indication that the large porous network due to spaces between the fibers is primarily responsible for superhydrophobicity and that pores on individual fibers play a minimal role.

This research is sponsored by the Defense Advanced Research Projects Agency (DARPA), contract number W91CRB10⁻¹-0003, technical sponsor Captain Christopher Warren, USN. The content of this article does not necessarily reflect the position or the policy of the Government, and no official endorsement should be inferred.

References

1. Rothstein, J. P. *Annu Rev Fluid Mech* 2010, 42, 89.
2. Shirtcliffe, N. J.; Hale, G.; Newton, H. I.; Perry, C. C. *Langmuir* 2003, 19, 5626.
3. Erbil, H. Y.; Demirel, A. L.; Avci, Y.; Mert, O. *Science* 2003, 299, 1377.
4. Love, J. C.; Gates, B. D.; Wolfe, D. B.; Paul, K. E.; Whitesides, G. M. *Nano Lett* 2002, 2, 891.
5. Fresnais, J.; Chapel, J. P.; Poncin-Epaillard, F. *Surf Coat Technol* 2006, 200, 5296.
6. Pozzato, A.; Zilio, S. D.; Fois, G.; Vendramin, D.; Mistura, G.; Belotti, M.; Chen, Y.; Natali, M. *Microelectron Eng* 2006, 83, 884.
7. Shi, F.; Wang, Z. Q.; Zhang, X. *Adv Mater* 2005, 17, 1005.
8. Zhao, N.; Shi, F.; Wang, Z. Q.; Zhang, X. *Langmuir* 2005, 21, 4713.
9. Gad-el-Hak, M. *Flow Control: Passive, Active, and Reactive Flow Management*; Cambridge University Press: London, United Kingdom, 2000.
10. Sarkar, S.; Deevi, S.; Tepper, G. *Macromol Rapid Commun* 2007, 28, 1034.
11. Jiang, L.; Zhao, Y.; Zhai, J. *Angew Chem Int Ed Engl Suppl.* 2004, 43, 4338.
12. Ma, M.; Mao, Y.; Gupta, M.; Gleason, K. K.; Rutledge, G. C. *Macromolecules* 2005, 38, 9742.
13. Acatay, K.; Simsek, E.; Ow-Yang, C.; Menciloglu, Y. Z. *Angew Chem Int Ed* 2004, 43, 5210.
14. Jin, M.; Feng, X.; Feng, L.; Sun, T.; Zhai, J.; Li, T.; Jiang, L. *Adv Mater* 1997 2005, 17.
15. Krupenkin, T. N.; Taylor, J. A.; Schneider, T. M.; Yang, S. *Langmuir* 2004, 20, 3824.
16. Wang, S.; Song, Y.; Jiang, L. *Nanotechnology* 2007, 18, 015103.
17. Cassie, A. B. D.; Baxter, S. *Trans Faraday Soc* 1944, 40, 546.
18. Hoefnagels, H. F.; Wu, D.; de With, G.; Ming, W. *Langmuir* 2007, 23, 13158.
19. Chao-Hua, X.; Shun-Tian, J.; Jing, Z.; Li-Qiang, T.; Hong-Zheng, C.; Mang, W. *Sci Technol Adv Mater* 2008, 9, 035008.
20. Megelski, S.; Stephens, J. S.; Chase, D. B.; Rabolt, J. F. *Macromolecules* 2002, 35, 8456.
21. Casper, C. L.; Stephens, J. S.; Tassi, N. G.; Chase, D. B.; Rabolt, J. F. *Macromolecules* 2004, 37, 573.